Duan, M., Perdikaris, P.C., Chen, W. "Impact Effect of Moving Vehicles."
Bridge Engineering Handbook.
Ed. Wai-Fah Chen and Lian Duan
Boca Raton: CRC Press, 2000

56

Impact Effect of Moving Vehicles

Mingzhu Duan
Quincy Engineering, Inc.

Philip C. Perdikaris
Case Western Reserve University

Wai-Fah Chen
Purdue University

56.1 Introduction

Vehicles such as trucks and trains passing bridges at certain speeds will cause dynamic effects, among them global vibration and local hammer effects. The dynamic loads for moving vehicles are considered "impact" in bridge engineering because of the relatively short duration. The magnitude of the dynamic response depends on the bridge span, stiffness and surface roughness, and vehicle dynamic characteristics such as moving speed and isolation system. Unlike earthquake loads which can cause vibration in bridge longitudinal, transverse, and vertical directions, moving vehicles mainly excite vertical vibration of the bridge. Impact effect has influence primarily on the superstructure and some of substructure members above the ground because the energy will be dissipated effectively in members underground by the bearing soils.

Although the interaction between moving vehicles and bridges is rather complex, the dynamic effects of moving vehicles on bridges are accounted for by a dynamic load allowance, *IM,* in addition to static live load (*LL*) in the current bridge design specifications [1–3]. According to the American Association of State Highway and Transportation Officials (AASHTO) and the American Railway Engineering Association (AREA) specifications,

$$IM = \frac{D_{dyn}}{D_{st}} - 1 \tag{56.1}$$

where D_{dyn} is the maximum dynamic response for deflection, moment, or shear of the structural members and D_{st} is the corresponding maximum static response. The total live-load effect, *LL,* can then be expressed as

$$LL = AF \times D_{st} \tag{56.2}$$

and

$$AF = 1 + IM \tag{56.3}$$

where *AF* is the amplification factor representing the dynamic amplification of the static load effect and *IM* is the impact factor determined by an empirical formula in design code. No dynamic analysis is thus required in the design practice.

Most early research work on the dynamic bridge behavior of bridges under moving vehicles focused on an analytical approach modeling a bridge as a simply supported beam [5] or a simply supported plate [8] under constant or pulsating moving loads (moving load model). The dynamic effects under different speeds of the moving loads and different damping ratios were studied. It was found that the speed of vehicles and the fundamental period of the bridge dominate the dynamic behavior of the bridge. Since most bridges consist of both beams and plates such as girder deck bridges, the above simplified model has limited validity. Along with analytical study, numerical methods such as finite-element analysis and the finite-difference method have been used recently in studying the dynamic response of a vehicle–bridge system [10,21]. Two sets of equations of motion were developed for the bridge and vehicle, respectively. These equations are coupled at the contacting points between bridge and vehicle and the contact points are time and space dependent due to vehicles moving along a rough surface. An iteration procedure should be used to solve the coupled equations. Field measurements are another alternative to investigate the dynamic effect [13] which disclosed the range of live-load effect for steel I-girder bridges under truck load.

Based on analytical analysis and field measurement studies, major characteristics of the bridge dynamic response under moving vehicles can be summarized as follows:

1. Measured impact factors [13], *IM,* on highway bridges vary significantly, e.g., with the mean of about 0.12 and the standard deviation of about 0.05 for steel I-girder bridges. The measured impact factors are well below those of the AASHTO specifications.
2. Impact factor increases as vehicle speed increases in most cases.
3. Impact factor decreases as bridge span increases.
4. Under the conditions of "very good" road surface roughness (amplitude of highway profile curve is less than 1 cm), the impact factor is well below that in design specifications. But the impact factor increases tremendously with increasing road surface roughness from "good" to "poor" (the amplitude of highway profile curve is more than 4 cm) and can be well beyond the impact factor in design specifications.
5. Impact factor decreases as vehicles travel in more than one lane. The chance of maximum dynamic response occurring at the same time for all vehicles is small.
6. Impact factor for exterior girders is much larger than for interior girders because the excited torsion mode shapes contribute to the dynamic response of exterior girders.
7. The first mode shape of the bridge is dominant in most cases, especially for the dynamic effect in the interior girder in single-span bridges.

The impact factor, *IM,* is a well-accepted measurement for the dynamic effect of bridges under moving vehicles and is used in design specifications worldwide. Consideration of impact effect for highway and railway bridges in design practice will be introduced through examples in Sections 56.2 and 56.3, respectively. Free vibration and forced vibration by a moving vehicle will be introduced in Sections 56.4 and 56.5 to disclose the dynamic behavior of the bridge vibration.

56.2 Consideration of Impact Effect in Highway Bridge Design

Since the impact effect on bridges by moving vehicles is influenced by factors such as bridge span, stiffness, surface roughness, and speed and suspension system of moving vehicles, the impact factor

varies within a large range. While the actual modeling of this effect is complex, the calculation of impact effect is greatly simplified in the bridge design practice by avoiding any analysis of vehicle-induced vibration. In general, the dynamic effect is contributed by two sources: (1) local hammer effect by the vehicle wheel assembly riding surface discontinuities such as deck joints, cracks, delaminations, and potholes; and (2) global vibration caused by vehicles moving on long undulations in the roadway pavement, such as those caused by settlement of fill, or by resonant excitation of the bridge. The first source has a local impact effect on bridge joints and expansions. On the other hand, the second source will have influence on most of the superstructure members and some of the substructure members. A variety of considerations and design formulas are proposed worldwide for the second source, which means that the bridge community has not reached a consensus on this issue [4]. The differences among various code specifications worldwide for the dynamic amplification factor vs. the fundamental frequency are large. A large dynamic effect is considered in some countries for the bridge frequency ranging from 1.0 to 5.0 Hz, which is the frequency range of the fundamental frequencies of most truck suspension systems. It is largely an attempt to penalize the bridge designed within this frequency range. But the accurate evaluation of the first frequency of a bridge can be hardly performed in the design stage.

In the AASHTO *Standard Specifications of Highway Bridges* (1996) in the United States, the impact factor due to bridge vibration for members in Group A including superstructure, piers, and those portions of concrete and steel piles above the ground that support the superstructure, is simply expressed as a function of bridge span:

$$IM = \frac{50}{L + 125} \leq 0.30 \tag{56.4}$$

where L (in ft) is the length of span loaded to create maximum stress.

In the AASHTO *LRFD Bridge Design Specifications* (1994), the static effects of the design truck or tandem shall be increased by the impact effect in the percentage specified in Table 56.1.

In Table 56.1, 75% of the impact effect is considered for deck joints for all limit states due to local hammer effect, 15% for fatigue and fracture limit states for members vulnerable to cyclic loading such as shear connectors and welding members, and 33% for all other members influenced by global vibration. Field tests indicate that in the majority of highway bridges, the dynamic component of the response does not exceed 25% of the static response to vehicles. Since the specified live-load combination of the design truck and lane load represents a group of exclusion vehicles which are at least ⅔ of those caused by the design truck alone on short- and medium-span bridges, the specified value of 33% in Table 56.1 is the product of ⅔ and the basic 25%. The impact effect is not considered for retaining walls not subjected to vertical reactions from superstructure, and for underground foundation components due to the damping effect of soil.

The dynamic effect caused by vehicles is accounted for in bridge design practice in the live-load calculation, as shown in the following example.

Example 56.1 — Live-Load Calculation in Highway Bridge Design

Given

The bridge shown in Figure 56.2 is a steel girder-concrete deck bridge with a span of 50 ft (15.24 m). The bridge carrying two lanes of traffic loads consists of four girders with girder-to-girder spacing of 7 ft (2.13 m). The steel girders are W36 × 150 and the average concrete deck thickness is 9 in. (3.54 m). The bridge is designed to carry a specified truck of HS20-44.

Solution 1

Using AASHTO *Standard Specifications of Highway Bridges* (1996) to calculate the design live-load moment for the interior steel girder under design truck HS20-44.

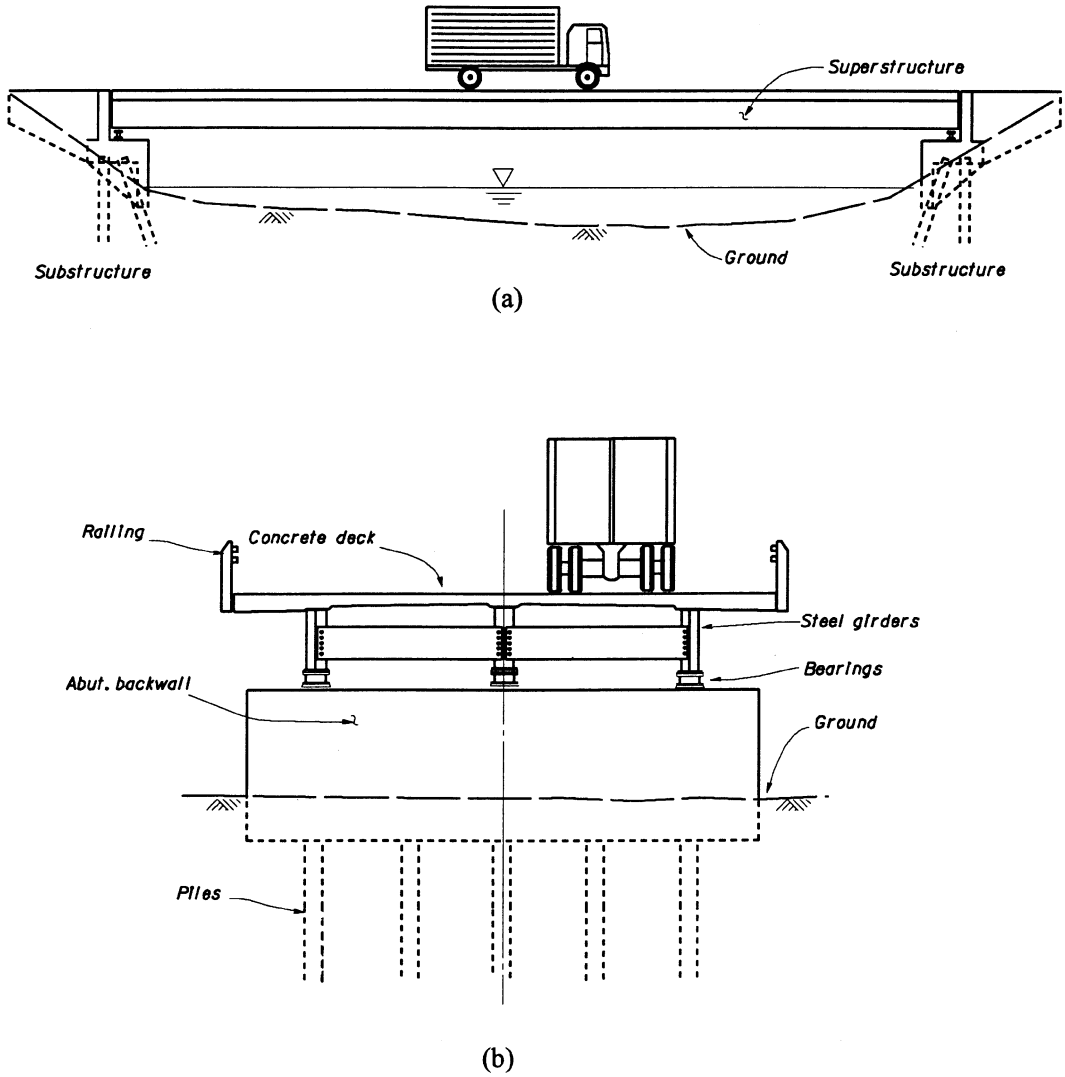

FIGURE 56.1 (a) Moving vehicle on a bridge. (b) Section view of the bridge and the vehicle.

TABLE 56.1 Dynamic Load Allowance, *IM*

Component	*IM*
Deck joint — All limit states	75%
All other components:	
• Fatigue and fracture limit state	15%
• All other limit states	33%

1. **Calculate the Static Design Moment in the Interior Stringer under Truck HS20-44**
   a. *Compute the static maximum truck load moment in a lane at the critical section of the superstructure induced by truck loading*:
   There are two types of vehicle live loading: truck and lane loading. For bending moments caused by HS20-44 loading for a span length of up to 140 ft, truck loading will govern.

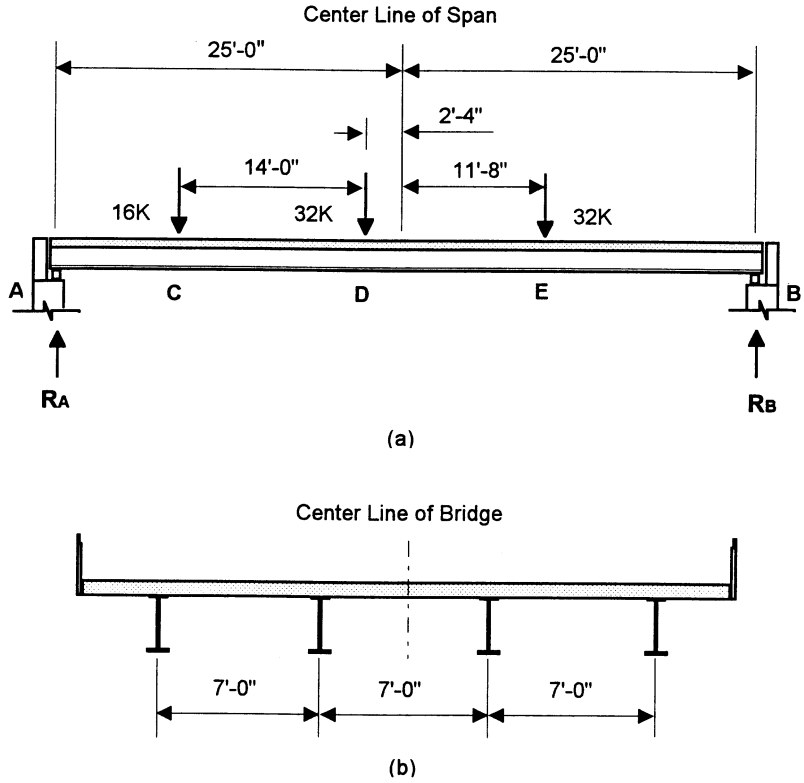

FIGURE 56.2 (a) Elevation of the steel girder bridge under truck load HS20-44. (b) Section of the steel girder bridge.

The maximum live-load moment is induced at the most adverse truck position. In fact, the maximum moment occurs at the position of the second concentrated load when the centerline of the span is midway between the center of gravity of loads and the second concentrated load as shown in Figure 56.2a. The reaction R_A at the end A is determined by using the equilibrium equation of the sum of the moments about point B:

$$\sum M_B = 0$$

Thus,

$$50\ R_A - 8\ \times\ 41.33 - 32\ \times\ 27.33 - 32\ \times\ 13.33 = 0, \text{ and}$$

$$R_A = \frac{1632}{50} = 32.64 \text{ kip } (145.25 \text{ kN})$$

The maximum live-load moment at Point D (see Figure 56.2) is

$$M_{\max} = 22.67\ R_A - 8\ \times\ 4 = 627.95 \text{ kips-ft } (851.50 \text{ kN-m})$$

b. *Compute the axle load distribution factor, DF, for the stringers*:
For the two lane concrete floor with steel I-beam girders spacing at 7 ft (2.13 m), the distribution factor, *DF*, according to the AASHTO-96 is

$$DF = \frac{S}{2 \times 5.5} = \frac{7}{2 \times 5.5} = 0.64$$

c. *Calculate the design static bending moment in a stringer*:

$$M_{LL} = DF(M_{\max}) = 627.95 \times 0.64 = 401.89 \text{ kips-ft } (544.96 \text{ kN-m})$$

2. Determine Dynamic Amplification Factor, *AF*

$$AF = 1.0 + IM = 1.0 + \frac{50}{L + 125} = 1.0 + \frac{50}{50 + 125} = 1.29 \quad \text{(AASHTO-96)}$$

3. Calculate the Total Bending Moment under Live Load

The total live bending moment including the amplification factor is

$$M_{LL+IM} = M_{LL}\, AF$$

$$= 401.89 \times 1.29 = 518.44 \text{ kips-ft } (703.00 \text{ kN-m}) \quad \text{(AASHTO-96)}$$

Solution 2

Using AASHTO-LRFD *Design Specifications* (1994) to calculate the design live-load moment for an interior steel girder under truck HS20-44.

1. Calculate the Static Truck Moment in the Interior Girder under Truck HS20-44

a. *The maximum moment in a lane is the same as in Method 1*:

$$M_{\max} = 627.95 \text{ kips-ft} \quad (851.50 \text{ kN-m})$$

b. *Compute the moment load distribution factor, DF, for the steel girders*:
For the two-lane concrete floor with steel I-girders spacing at 7 ft (2.13 m), the distribution factor, *DF*, is

$$DF = 0.075 + \left(\frac{S}{9.5}\right)^{0.6}\left(\frac{S}{L}\right)^{0.2}\left(\frac{K_g}{12.0\, Lt_s^3}\right)^{0.1} = 0.075 + \left(\frac{7.0}{9.5}\right)^{0.6}\left(\frac{7.0}{L}\right)^{0.2} \times 1.0 = 0.63$$

(for preliminary design use)

c. *Calculate the design static bending moment in a stringer*:

$$M_{LL} = DF(M_{\max}) = 627.95 \times 0.63 = 395.64 \text{ kips-ft } (538.07 \text{ kN-m})$$

2. Determine Dynamic Amplification Factor, *AF*

$$AF = 1.0 + IM = 1.0 + 0.33 = 1.33 \quad \text{(AASHTO-94)}$$

3. Calculate the Total Bending Moment in an Interior Stringer under Truck Load

The total bending moment under truck load including the amplification factor is

$$M_{LL+IM} \text{ (truck)} = M_{LL}\, AF = 395.64 \times 1.33 = 526.20 \text{ kips-ft } (715.64 \text{ kN-m}) \quad \text{(AASHTO-94)}$$

4. The vehicular live-load moment is the combination of the design truck load with impact allowance and design lane load without impact allowance (0.64 kip/ft over 10.0 ft per lane, 0.88 kN/m over 3.0 m):

$$M_{LL+IM}\ (\text{total}) = 526.20 + 0.63 \times (0.64 \times 50/2 \times 22.67 - 1/2 \times 0.64 \times 22.67^2)$$
$$= 651.10\ \text{kips-ft}\ (885.50\ \text{kN-m})$$

56.3 Consideration of Impact Effect in Railway Bridge Design

For railway bridges the ratio of live load caused by moving vehicles such as locomotive and trains to the dead load is mostly higher than that in highway bridges. Similarly, as in highway bridge design, static live-load effect by vehicles should be increased by the impact factor to account for the dynamic amplification effect. The most important sources of bridge impact are

1. Initial vehicle bounce and roll,
2. Vehicle speed, and
3. Bridge dynamic properties and track-surface roughness.

In the AREA specifications [3], the impact loads specified are based on investigations and tests of railroad bridges in service under passage of locomotive and train loads. The vibration for the bridge is the most dominant dynamic effect in railway bridge design. In the vibration, the vertical vibration effect will be coupled with the rocking effect (*RE*) caused by vehicle pitch movement (transverse vehicle rotation). Thus, a couple with 10% of axle load acting down on one rail and up on the other rail should be added into the vertical impact effect. The rocking effect, *RE,* should be expressed as a percentage; either 10% of the axle load or 20% of the wheel load. The total impact effect can be calculated as

1. Percentage of live load for rolling equipment without hammer blow, such as diesels and electric locomotives, etc.,

$$IM = RE + 40 - \frac{3L^2}{1600} \qquad \text{if } L < 50\ \text{ft}\ (15.24\ \text{m})$$
$$IM = RE + 16 - \frac{600}{L - 30} \qquad \text{if } L \geq 80\ \text{ft}\ (24.39\ \text{m}) \tag{56.5}$$

2. Percentage of live load for steam locomotives with hammer blow:
   a. For beam spans, stringers, girders, floor beams, parts of deck truss span carrying load from floor beam only:

$$IM = RE + 40 - \frac{L^2}{500} \qquad \text{if } L < 100\ \text{ft}\ (30.48\ \text{m})$$
$$IM = RE + 10 - \frac{1600}{L - 40} \qquad \text{if } L \geq 100\ \text{ft}\ (30.48\ \text{m}) \tag{56.6}$$

   b. For truss spans:

$$IM = RE + 10 - \frac{4000}{L + 25} \tag{56.7}$$

where L is the effective span length (ft).

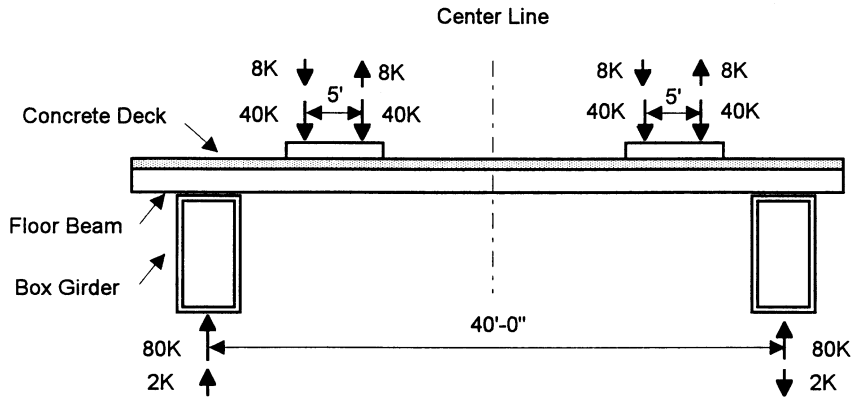

FIGURE 56.3 Rocking effect model for railway bridge.

Tests have shown that the impact load on ballasted deck bridges can be reduced to 90% of that specified for open-deck bridges because of the damping effect which results from a ballasted deck bridge. It was found from a parametric study [9] that the impact ranges from 24.9 to 26.0%, with an average of 25.6%, except for hangers. The following example shows how to account for impact effect in live-load calculation in railway bridge design.

Example 56.2 — Live Load Calculation in Railway Bridge Design

Given

A ballasted 105-ft-long (32.01-m-long) deck bridge is supported by two box girders. The box girder spacing is 40 ft (12.20 m) to carry two tracks, as shown in Figure 56.3. Live load is Cooper E-80 without hammer blow. The maximum bending moment M_{LL} at midspan under static live load is 15,585 kips-ft (21,195.60 kN-m) per track based on AREA values. The bending moment M_{LL+IM} at midspan under live load can be calculated as follows.

1. **Determine Rocking Effect (*RE*)**

   The maximum axle load is 80 kips (356.00 kN) (40 kips per rail, 178.00 kN per rail).

   The couple force generated by the rocking effect:

   $$20\% \times 40 = 8 \text{ kip } (35.60 \text{ kN})$$

   The total couple force at the box girders is:

   $$\text{total couple} = 8 \times 5 \text{ ft (rail spacing)} \times 2 \text{ tracks} = 40 \text{ kips-ft } (54.24 \text{ kN-m})$$

   $$\text{total couple force} = \frac{\text{total couple}}{\text{stringer spacing}} = \frac{80}{40} = 2.0 \text{ kip } (8.9 \text{ kN})$$

   The rocking effect on the stringers is the ratio of rocking reaction to static reaction:

   $$RE = \frac{2.0}{80} = 0.025 = 2.5\%$$

2. **Determine the Percentage of Impact Effect from AREA Specifications**

   For $L > 80$ ft (24.39 m) and no hammer effect case:

   $$IM = RE + \left(16 + \frac{600}{L - 30}\right)\% = 2.5 + \left(16 + \frac{600}{108 - 30}\right)\% = 26.21\%$$

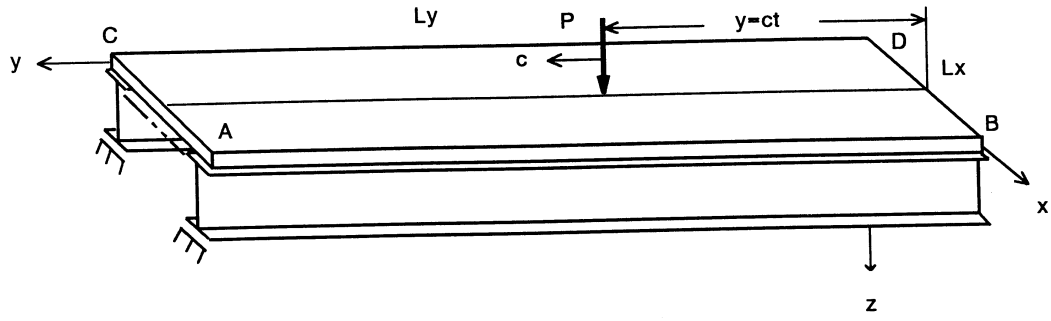

FIGURE 56.4 Girder deck bridge under moving constant load.

For ballasted deck bridges, 90% reduction should be considered, that is:

$$IM = 90\% \times 26.21\% = 0.24$$

3. Determine Live-Load Effect of the Maximum Bending Moment at Midspan

$$AF = 1.0 + IM = 1.0 + 0.24 = 1.24$$

$$M_{\mathrm{LL+IM}} = AF\ (M_{LL}) = 1.24 \times 15{,}585 = 19{,}264 \text{ kips-ft } (26{,}199.04 \text{ kN-m})$$

56.4 Free Vibration Analysis

56.4.1 Structural Models

In the following two sections, the bridge vibration under moving load will be discussed to investigate the dynamic response of bridges. There have been basically two types of analysis methods: numerical analysis (sprung mass model) and analytical analysis (moving load model). The numerical analysis models the interaction between vehicle and bridge and expresses the dynamic behavior numerically. On the other hand, analytical analysis greatly simplifies vehicle interaction with bridge and models a bridge as a plate or beam but expresses the dynamic behavior explicitly. Good accuracy can be obtained using the analytical model when the ratio of live-load to self-weight of the superstructure is less than 0.3. The analytical analysis method will be presented for a bridge with beam-plate system.

The structure shown in Figure 56.4 represents a plate with two opposite edges AC and BD simply supported by rigid ground and the other two edges AB and CD simply supported on two beams. The assumptions made are

a. The stress–strain relationship for the beam and plate material is linear elastic;
b. There exists a neutral plane surface in the plate and the existence of the beams does not have any influence on the position of this neutral plane, i.e., the beam can only provide a vertical force reaction to the edges AB and CD for the plate. The structure is a noncomposite girder deck bridge; and
c. Thin plate and simple beam theories are applicable.

56.4.2 Free Vibration Analysis

The differential equation for free vibration of the plate shown in Figure 56.4 is

$$D\ \nabla^{(4)} W\ +\ m\ W_{tt}^{(2)}\ =\ 0 \tag{56.8}$$

where

$D = \dfrac{Eh^3}{12(1-\mu)}$ = the flexural rigidity of the plate
m = is the mass per unit area of the plate
W = is the vertical deflection of the plate

The boundary conditions for the plate are as follows:

At $y = 0$ and $y = L_y$:

$$W\ (x,\ y,\ t) = 0 \tag{56.9a}$$

$$M_y(x,\ y,\ t) = 0 \tag{56.9b}$$

At $x = 0$:

$$M_x\ (x,\ y,\ t) = 0 \tag{56.9c}$$

$$Q_x + \frac{\partial M_{xy}}{\partial y} = E_b I_b \frac{\partial^4 W}{\partial y^4} + m_b \frac{\partial^2 W}{\partial\, t^2} \tag{56.9d}$$

At $x = L_x$:

$$M_x\ (x,\ y,\ t) = 0 \tag{56.9e}$$

$$Q_x + \frac{\partial M_{xy}}{\partial y} = -E_b I_b \frac{\partial^4 W}{\partial y^4} - m_b \frac{\partial^2 W}{\partial t^2} \tag{56.9f}$$

where $E_b I_b$ and m_b is the flexural rigidity and mass per unit beam length, respectively, and M_x, M_y are the transverse and longitudinal bending moments, respectively. M_{xy} is the torque and Q_y is the shear force at the edges of the plate, respectively. Their signs are shown in Figure 56.5. The terms at the right-hand side in Eqs. (56.9d) and (56.9f) represent the interaction forces at the edges AB and CD between the plate and the beams. It is seen that the participation of the beams is taken into account in the partial differential equations through the boundary conditions for the plate.

Assuming that the structure vibrates in a mode so that the deflected shape is described by

$$W = \sin\frac{i\pi y}{L_y} X_j(x)\ \sin(\omega_{ij} t + q) \tag{56.10}$$

the following equations can be derived by substituting Eq. (56.10) into Eq. (56.8):

$$X_j^{(4)} - 2\frac{i^2\pi^2}{L_y^2} X_j^{(2)} + \frac{i^4\pi^4}{L_y^4} X_j - \frac{m}{D}\omega_{ij} X_j = 0 \tag{56.11}$$

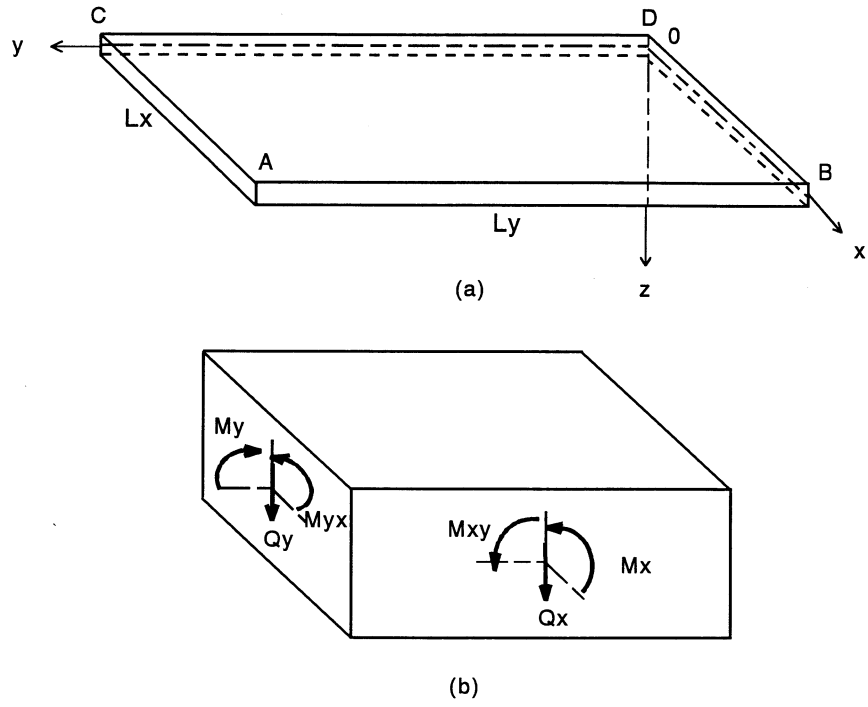

FIGURE 56.5 (a) A three-dimensional plate with length L_y and width L_x. (b) A volume element with inter forces acting on its sides.

The solution to the homogeneous differential equation above is

$$X_j = e^{\lambda\, x/Lx}$$

where λ must satisfy the characteristic equation:

$$\frac{l^4}{L_x^4} - 2\frac{i^2\pi^2}{L_y^2}\frac{l^2}{L_x^2} + \left(\frac{i^4\pi^4}{L_y^4} - \frac{m\omega_{ij}^2}{D}\right) = 0 \tag{56.12}$$

There are four roots for this equation. According to the signs of the roots, $X_j(x)$ will take two different forms, which will be discussed separately.

Case 1

$$i^2 > p r_{ij}^2$$

where

$$p r_{ij}^2 = \frac{\omega_{ij}^2 m L_y^2}{D\pi^4} \tag{56.13}$$

We have the following solution for Eq. (56.11)

$$X_j = \sinh \lambda_1 u + A\cosh \lambda_1 u + B\sinh \lambda_2 u + C\cosh \lambda_2 u$$
$$\lambda_{1,2} = \frac{\pi}{\gamma}\left[i^2 \mp pr_{ij}^2\right] \tag{56.14}$$

where

$$u = x/L_x \tag{56.15.a}$$

$$\gamma = L_y / L_x \tag{56.15.b}$$

By substituting Eq. (56.14) and (56.10) into the boundary conditions in Eqs. (56.9a) to (56.9f), the constants *A*, *B*, and *C* in Eq. (56.14) can be determined by solving a group of eigenvalue equations [7].

The natural frequency ω_{ij} in Case 1 can be obtained from the following nonlinear equation from the boundary conditions as

$$2\lambda_1\lambda_2 D_1^2 D_2^2(\cosh \lambda_1 \cosh \lambda_2 - 1) - \left(\lambda_1^2 D_1^4 + \lambda_2^2 D_2^4\right)\sinh \lambda_1 \sinh \lambda_2$$
$$-\left(D_1 + D_2\right)^2 Q^2 \sinh \lambda_1 \sinh \lambda_2 + 2Q(D_1 + D_2) \tag{56.16}$$
$$\left(\lambda_2 D_2^2 \sinh \lambda_1 \cosh \lambda_2 - \lambda_1 D_1^2 \cosh \lambda_1 \sinh \lambda_2\right) = 0$$

where

$$D_{1,2} = \frac{\pi^2}{\gamma^2}\left((1-\mu)i^2 + pr_{ij}^2\right)$$

$$Q = (E_b D_b \frac{i^4\pi^4}{L_y^4} - m_b\omega_{ij}^2) / D L_y^3$$

and *Q* in Eq. (56.16) represents the interaction between the plate and the beams.

Case 2

$$i^2 < pr_{ij}^2$$

In this case, the solution for Eq. (56.11) would be

$$X_j = \sin \lambda_1 u + A\cos \lambda_1 u + B\sinh \lambda_2 u + C\cosh \lambda_2 u \tag{56.17}$$

where

$$l_{1,2} = \frac{\pi}{\gamma}\left[pr_{ij}^2 \mp i^2\right]$$

By substituting Eqs. (56.17) and (56.11) into the boundary conditions in Eqs. (56.9a) to (56.9f), we can obtain the constants in Eq. (56.17) as in Case 1 by solving a group of eigenvalue equations [7].

The natural frequency ω_{ij} in Case 2 can be obtained from the following equation:

$$2\lambda_1\lambda_2 D_1^2 D_2^2(\cos\lambda_1\cosh\lambda_2 - 1) - \left(\lambda_1^2 D_1^4 + \lambda_2^2 D_2^4\right)\sin\lambda_1\sinh\lambda_2$$
$$-\left(D_1 + D_2\right)^2 Q^2 \sin\lambda_1\sinh\lambda_2 + 2Q(D_1 + D_2) \qquad (56.18)$$
$$\left(\lambda_2 D_2^2 \sin\lambda_1\cosh\lambda_2 - \lambda_1 D_1^2 \cos\lambda_1\sinh\lambda_2\right) = 0$$

Example 56.3 Free Vibration Analysis for a Beam-Plate Bridge

A one-lane bridge deck structure is shown in Figure 56.4. The plate is made of an isotropic material representing reinforced concrete, and the beams are made of steel with a W36 × 150 section. The bridge span length is 80 ft (24.39 m) and the bridge width is 10 ft (3.05 m). The thickness of the deck plate is 8 in. (3.15 cm). The elasticity modulus of the steel girder $E_b = 29.0 \times 10^3$ ksi (200.0×10^3 MPa) and the elasticity modulus of the concrete plate is $E = 4.38 \times 10^3$ ksi (30.18 MPa). The mass density of the plate $m = 0.8681$ lb/in.^{2} g (0.61 kN/cm^2 g) and the mass density of the beam is $m_b = 12.50$ lb/in.$^2 g$ (22.0 N/cm g) where g is the gravitational acceleration. The moment of inertia of the beam is $I_b = 9030$ in.^{4} (375,800 cm^4). All other properties are calculated as:

Bending rigidity of the plate in y direction:

$$L_x D = \frac{L_x E t^3}{12(1.0 - \mu)} = 4.56 \times 10^{10} \text{ lb.in.}^2 \ (1.28 \times 10^{12} \text{ kN.cm}^2)$$

Bending rigidity ratio between beam and plate:

$$R_{ej} = \frac{2.0 E_b I_b}{L_x D} = 11.5$$

Mass ratio between beam and plate:

$$R_m = \frac{m_b}{L_x m} = 0.12$$

First natural frequency of the plate as a beam:

$$\omega_{11}^p = \frac{p^2}{L_y^2}\sqrt{\frac{D}{m}} = 4.40 \text{ rad/s}$$

First natural frequency of the beam:

$$\omega_1^b = \frac{p^2}{L_y^2}\sqrt{\frac{E_b I_b}{m_b}} = 30.45 \text{ rad/s}$$

Subscripts i and j represent the ith and jth mode shape in the y- and x-direction, respectively. The natural frequencies, ω_{ij}, can be determined numerically using Eqs. (56.16) and (56.18). Some of the first several natural frequencies are shown in Table 56.2.

The mode shapes of the bridge are shown in Figures 56.6 and 56.7 using normalized dimensions in all three directions. It is seen that W_{12}, W_{14}, W_{22}, and W_{24} are all asymmetric mode shapes in the

TABLE 56.2 Natural Frequencies of One-Lane Bridge Deck (rad/s; plate aspect ratio = 8.0)

	$j=1$	$j=2$	$j=3$
$i=1$	14.53	35.43	482.65
$i=2$	60.09	110.62	506.27
$i=3$	125.67	217.44	556.53
$i=4$	206.05	354.98	647.51

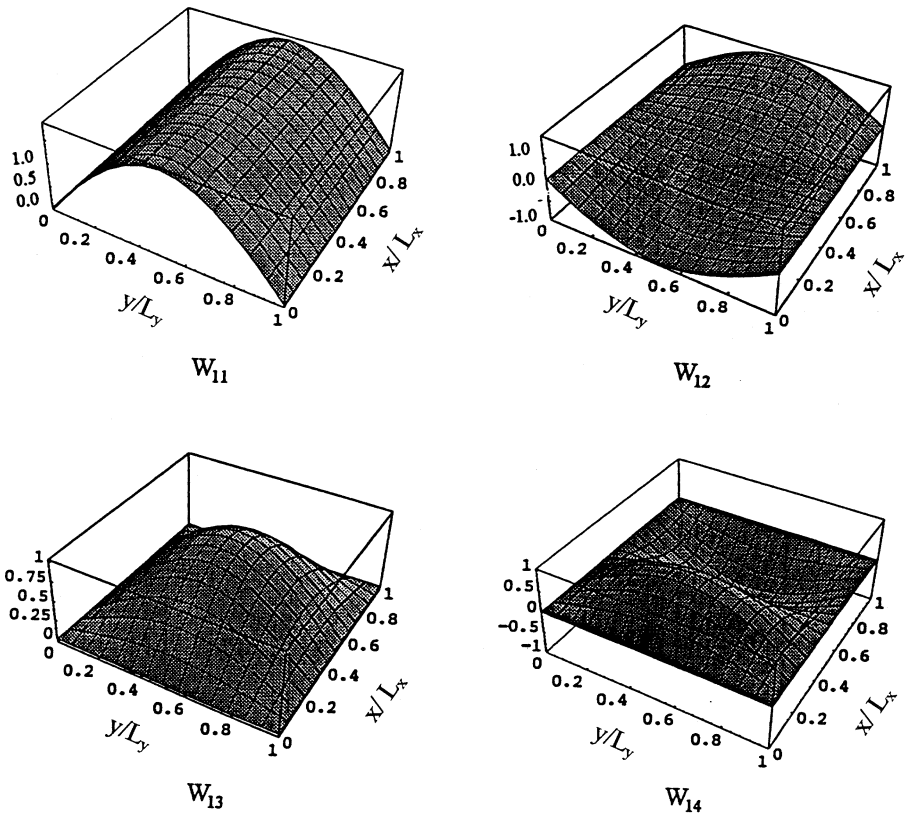

FIGURE 56.6 Normalized three-dimensional mode shapes W_{ij}, $i=1$, $j=1,2,3,4$, for a one-lane bridge deck. (subscripts i-j is the mode shape number in y- and x-directions, respectively).

x-direction about the center line $x = L_x/2$. When a moving load traverses the plate along this line, these mode shapes would not be excited. Thus, there are no contributions from these mode shapes.

The first mode shape of the beam–plate system is nearly a constant in the x-direction, as shown in this example of a rather high plate aspect ratio. This means that the beams have the same first mode shape as the plate. In this case, the first natural frequency of the beam–plate system can be approximately evaluated as

$$\omega_{11}^2 = \frac{2R_m\omega_1^{b\,2} + \omega_{11}^{p\,2}}{1+2R_m} \tag{56.19}$$

where ω_1^b and ω_1^p are fundamental frequencies of the beam and plate as a beam, respectively.

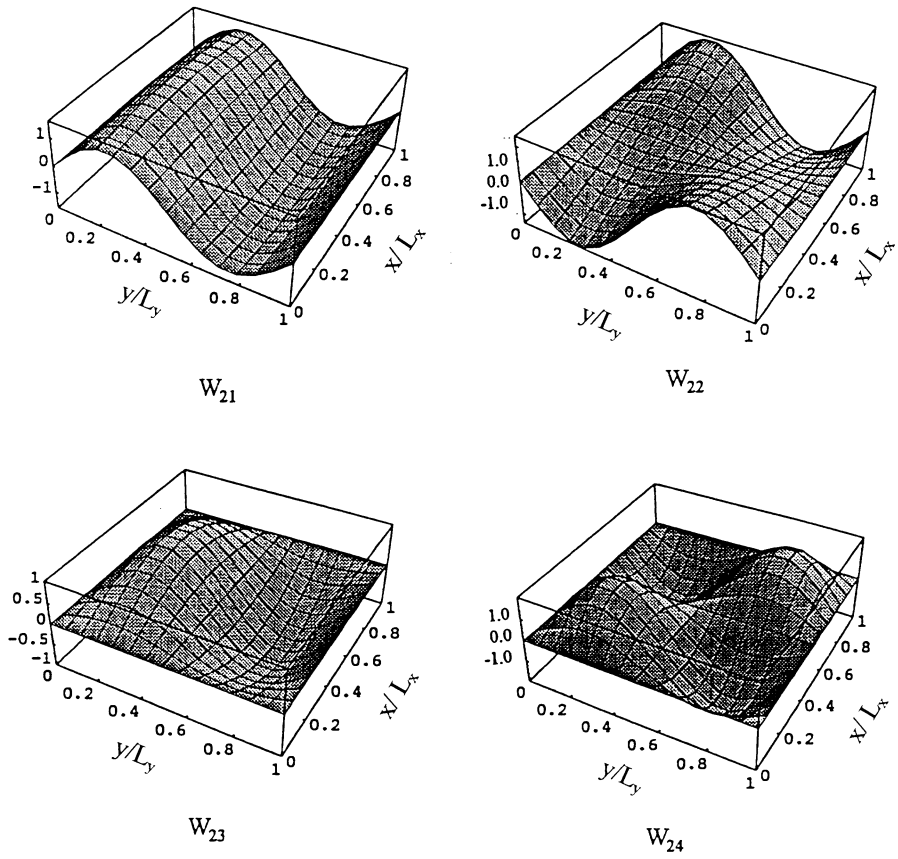

FIGURE 56.7 Normalized three-dimensional mode shapes W_{ij}, $i = 2$, $j = 1,2,3,4$, for a one-lane bridge deck (subscripts i-j is the mode shape number in y- and x-directions, respectively).

56.5 Forced Vibration Analysis under Moving Load

56.5.1 Dynamic Response Analysis

The governing equation for the plate with smooth surface supported by two beams under a moving constant load shown in Figure 56.4 is

$$\nabla^4 W + \frac{m}{D}\frac{\partial^2 W}{\partial t^2} = \frac{1}{D}p(x,y,t) \quad (0 < t < L_y/c) \tag{56.20}$$

where

$$p(x,y,t) = P\,\delta(y - ct)\,\delta(x - L_x/2)$$

and c is the speed of the moving load, and P the magnitude of the moving load. A Dirac delta function represents a unit concentrated force acting on the deck.

The method of modal superposition is used to get the dynamic response by assuming

$$W = \sum_{i=1}^{+\infty} \sum_{j=1}^{+\infty} W_{ij}(t) \sin \frac{i\pi y}{L_y} X_j(x) \tag{56.21}$$

By substituting Eq. (56.21) into Eq. (56.20), the following ordinary differential equation can be derived:

$$W_{ij,t}^{(2)}(t) + 2\xi_{ij}\omega_{ij} W_{ij,t}^{(1)} + \omega_{ij}^2 W_{ij} = \frac{2P}{m L_x L_y} X_{ij}(L_x/2) \sin \frac{i\pi c}{L_y} t \quad (0 < t < L_y/c) \tag{56.22}$$

where ξ_{ij} is the damping ratio for mode shape *i–j*. The initial condition is that the bridge structure is in a static state before the load enters the span and the structure is in a state of free vibration after the load traverses the bridge.

There are several parameters affecting the dynamic response of the structure. The influence of some typical parameters such as the speed of the moving load and damping ratio is presented in the following.

The vehicle speed is normalized as

$$\alpha = \frac{\pi c / L_y}{\omega_{11}} \tag{56.23}$$

For example, if the load is moving at a speed of 60 mph, the span of the bridge is 80 ft and first natural frequency is 14 Hz, the normalized speed is $\alpha = 0.25$. A normalized speed of $\alpha = 0.5$ represents the case for which the time needed for a vehicle to traverse the span is the same as the first period of the bridge. Typical normalized dynamic deflections are shown in Figure 56.8. It is seen that for the normalized speed ranging $0 < \alpha < 1.0$, the maximum deflection occurs when the load is on the bridge while if $\alpha > 1.0$, the maximum deflection occurs after the load traverses the bridge. When the load is on the plate ($ct/L_y < 1.0$), the deflections at the center are usually positive. But the deflections are negative after the load has traversed the plate ($ct/L_y > 1.0$), especially for the case of $0 < \alpha < 0.5$. The change of sign for deflection results in a curvature change and, hence, in a stress sign change.

The normalized deflection at the center of the plate is defined as the dynamic deflection caused by moving constant load divided by the corresponding static deflection caused by the concentrated constant force. Figure 56.9 shows its spectra for an aspect ratio of 8.0. The normalized speed of the moving load affects the maximum dynamic response significantly. For small α values, e.g., less than 0.20, which refers to long-span bridges or slow-speed vehicle, there is little dynamic amplification. Very low speed values or very long bridges do not result in much dynamic response. When the normalized speed is greater than 1.3, corresponding to very short span bridges, the dynamic effect is also not significant because the duration of excitation is extremely short. The maximum dynamic response happens for normalized speeds ranging from 0.45 to 0.65, when load frequency is near the bridge fundamental frequency. It is also found that the maximum bending moment amplification factors are 1.2 for M_y and 1.1 for M_x at a normalized speed of 0.4, while the maximum deflection amplification is about 1.5 at a normalized speed of 0.55. The dynamic amplification for bending moments is less than the dynamic amplification for deflections.

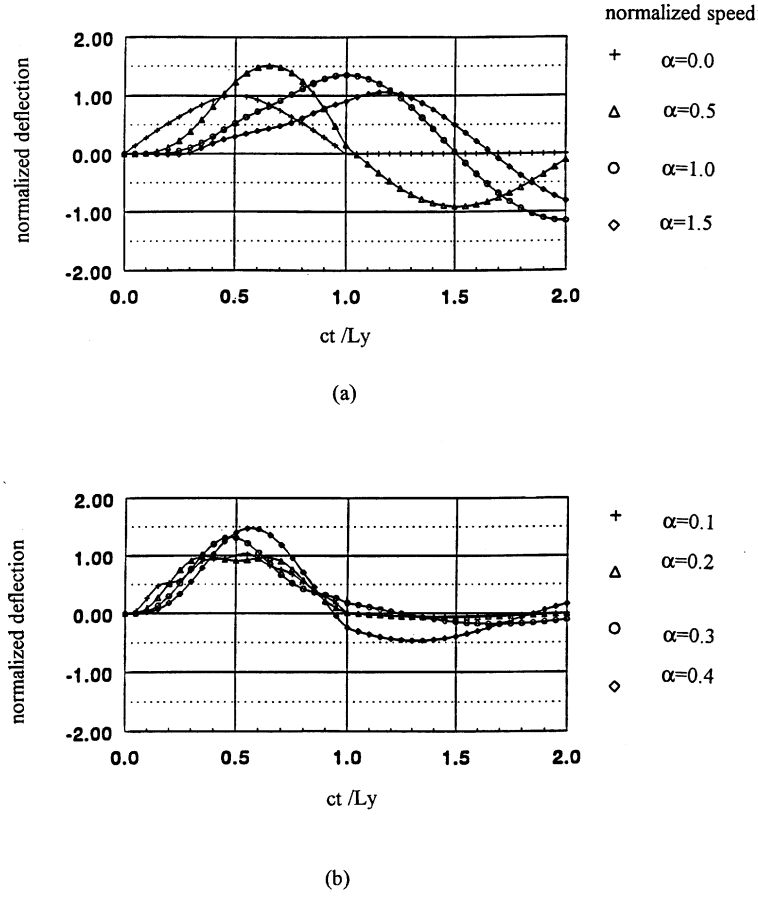

FIGURE 56.8 (a) Normalized deflections at the center of the deck with normalized speed, α = 0.0, 0.5, 1.0, and 1.5. (b) Normalized deflections at the center of the deck with normalized speed, α = 0.1, 0.2, 0.3, and 0.4.

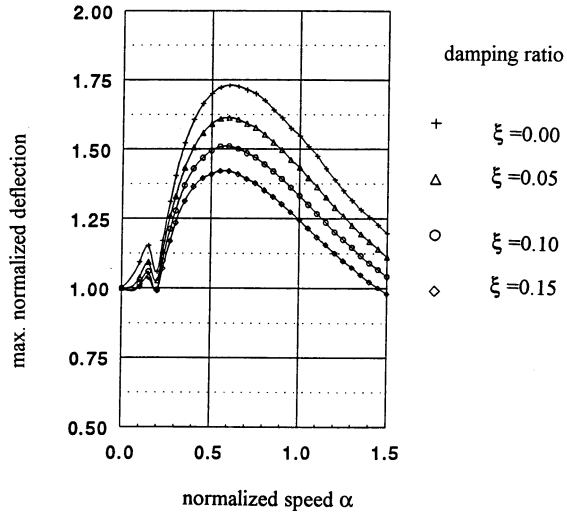

FIGURE 56.9 Normalized deflection spectra at the center of the deck for different damping ratios and normalized speeds.

56.5.2 Summary of Bridge Impact Behavior

For one-lane bridge deck structures, the conclusions of impact behavior of the bridge under moving constant loads have been drawn as:

1. The maximum deflection occurs when the moving load traverses the deck at a normalized speed less than 1.0, and the maximum deflection occurs when the load passes the deck at a normalized speed larger than 1.0.
2. The maximum impact effect is mostly expected when the duration of moving vehicle is close to the fundamental period of the bridge.
3. The aspect ratios of the deck play an important role. When they are less than 4.0, the first mode shape is dominant, when more than 8.0, other mode shapes are excited. The contributions from higher natural frequency mode shapes decrease slowly due to the fact that the natural frequency, ω_{ij}, increases slowly as subscript i increases. Thus, a sufficient number of terms of superimposed mode shapes are needed to get more accurate results.
4. Dynamic amplification for deflections is larger than for bending moments. The response curves of deflections are "smoother" than the response curves for bending moments in the time domain.
5. The dynamic response of a plate with two edges free and the other two edges simply supported is close to a beam for aspect ratios of the plate larger than 2.0.
6. The analysis of a moving constant load model usually overestimates the dynamic effect because vehicle mass is not considered in the dynamic analysis and thus overestimates the first frequency of the bridge–vehicle system which corresponds to the "shorter-span" bridge.

Acknowledgments

The authors would like to express their gratitude to Prof. Dario Gasparini for his endeavors and opinions and to the financial support from Case Western Reserve University in performing the dynamic analysis. Mr. Kang Chen, MG Engineering, Inc. provided valuable information for the railway bridge part, which is greatly appreciated.

References

1. AASHTO, *LRFD Bridge Design Specifications*, American Association of State Highway and Transportation Officials, Washington, D.C., 1994.
2. AASHTO, *Standard Specifications for Highway Bridges*, 16th ed., American Association of State Highway and Transportation Officials, Washington, D.C., 1996.
3. AREA, *Manual for Railway Engineering,* American Railway Engineering Association, Washington, D.C., 1996.
4. Barker, R. M. and Puckett, J. A., *Design of Highway Bridges — Based on AASHTO LRFD, Bridge Design Specifications,* John Wiley & Sons, New York, 1996.
5. Biggs, J. M., *Introduction to Structural Dynamics under Moving Loads,* McGraw-Hill, New York, Inc., 1964.
6. Chang, D. and Lee, H., Impact factors for simple-span highway girder bridges, *J. Struct. Eng. ASCE,* 120(3), 880–889, 1994.
7. Duan, M., Static Finite Element and Dynamic Analytical Study of Reinforced Concrete Bridge Decks, M.S. thesis, Department of Civil Engineering, Case Western Reserve University, Cleveland, OH, 1994.
8. Fryba, L., *Introduction to Structural Dynamics*, Groningen Noordhoff Futern, 1972.
9. Garg, V. K., *Dynamics of Railway Vehicle Systems*, Harcourt Brace Jovanovich, New York, 1984.
10. Huang, D., Wang, T.-L., and Shahawy, M., Impact analysis of continuous multi-girder bridges due to moving vehicles, *J. Struct. Eng. ASCE,* 118(12), 3427–3443, 1992.

11. Hino, J., Yoshimura, T., and Konishi, K., A finite element method prediction of the vibration of a bridge subjected to a moving vehicle load, *J. Sound Vibration,* 96(6), 45–53, 1984.
12. Huang, D., Wang, T.-L., and Shahawy, M., Vibration of thin-walled box-girder bridges exited by vehicles, *J. Struct. Eng. ASCE,* 121(9), 1330–1337, 1995.
13. Kim, S. and Nowak, A., Load distribution and impact factors for I-girder bridges, *J. Bridge Eng. ASCE,* 2(3), 1997.
14. Lin, Y. H. and Trethewey, M. W., Finite element analysis of elastic beams subjected to moving loads, *J. Sound Vibration*, 136(2), 323–342, 1990.
15. Petrou, M. F., Perdikaris, P. C., and Duan, M., Static behavior of noncomposite concrete bridge decks under concentrated loads, *J. Bridge Eng. ASCE,* 1(4), 143–154, 1996.
16. Scheling, D. R., Galdos, N. H., and Sahin, M. A., Evaluation of impact factors for horizontally curved steel box bridges, *J. Struct. Eng. ASCE,* 118(11), 3203–3221, 1992.
17. Timoshenko, S. P. and Woinowsky-Krieger, S., *Theory of Plates and Shells*, 2nd ed., McGraw-Hill, New York, 1959.
18. Wang, T.-L., Huang, D., and Shahawy, M., Dynamic response of multi-girder bridges, *J. Struct. Eng. ASCE,* 118(8), 2222–2238, 1992.
19. Xanthakos, P., *Theory and Design of Bridges*, John Wiley & Sons, New York, 1994.
20. Yang, Y.-B. and Lin, B.-H., Vehicle-bridge interaction analysis by dynamic condensation method, *J. Struct. Eng. ASCE,* 121(2), 1636–1643, 1995.
21. Yang, Y.-B. and Yau, J.-D., Vehicle-bridge interaction element for dynamic analysis, *J. Struct. Eng. ASCE,* 118(11), 1512–1518, 1997.